High-Sensitivity In-Situ Soot Particle Sensing in an Aero-Engine Exhaust Plume Using Long-Pulsed Fiber-Laser Induced Incandescence

David McCormick, *Member, IEEE*, John D. Black, Yutong Feng, Johan Nilsson and Krikor B. Ozanyan, *Senior Member, IEEE*

***Abstract*— A method to produce spatially resolved images of the distribution of absorbing particles in the exhaust plume of a modified helicopter gas turbine engine is presented. Over a small region of the plume, in-situ sensing of soot particles by Laser-Induced Incandescence (LII) is demonstrated using fiber-lasers with higher power (~10 W), longer pulse duration (>100 ns), and higher pulse repetition rates (>10 kHz) than conventional LII. The sensitivity of the method is illustrated by the detection of ambient absorbing particles in background conditions with engine at rest. With a running engine, single beam images are obtained in 0.01 s. The feasibility of using long-pulsed fiber-lasers for soot particle concentration measurement is investigated using a representative laboratory system. The time-resolved LII behavior and measurement linearity are investigated, demonstrating the suitability of using fiber-lasers for soot particle measurement for aero-engine emissions. Results for normalized soot concentration are compared with extractive measurements illustrating good correlation across a range of engine speeds. This work is the first step towards the development of a non-intrusive system for measurement of 2-D soot concentration in the cross-section of an aero-engine exhaust plume.**

***Index Terms*— aero-engine, fiber-laser, exhaust plume, laser induced incandescence, soot sensing, ambient sensing**

I. INTRODUCTION

Modern aero-engines emit only a small proportion of their total emissions in the form of solid particulates. However there are concerns about the effect these particulates have on air quality [1], their impact on human health because of their small size [2], and their potentially disproportionate effect on climate change [3]. Accurate measurement of soot concentration and distribution in aero-engine exhaust plumes is of interest to the aerospace engineering community because of the need to develop methods shown to meet engine certification standards. These can be used on new engines that have reduced environmental impact and are capable of burning sustainable fuels [4]. In addition to the environmental factors, measurement of soot emissions is a useful method for indicating the health of an aero-engine, where changes in soot concentration or its distribution across the plume can be an early indicator of a problem requiring further investigation [5].

Current requirements for emissions certification necessitate measurements of the SAE smoke number (SAESN) [6]. This method is an extractive sampling technique which uses a rake of probes positioned in the exhaust plume of a running engine. A volume of gas from the engine is passed through filter paper and the reflectance of the filter paper is measured to determine the SAESN. Although extractive measurements using the SAESN are well-established, they are time consuming and expensive, requiring the engine to be held in constant running condition for approximately 5 minutes for each measurement. Practical problems associated with extractive sampling include the need to develop probes that can withstand the harsh conditions of an aero-engine exhaust plume, and measurement uncertainties which arise when particulates aggregate on the surfaces of the probes and transfer lines.

Since modern aero-engines are considerably cleaner than when the SAESN measurement was introduced in the 1960s, the low levels of soot will often fail to register any significant change in reflectance of the filter paper, particularly at low engine power conditions. This problem is further exacerbated by modern synthetic and bio-fuels which produce less smoke than conventional oil-derived fuels. The limitations of current extractive techniques illustrate the need to investigate methods for rapid, cost-effective, and non-intrusive methods for sensing and measurement of aero-engine soot particulates [7].

A. *Laser Induced Incandescence*

Laser-Induced Incandescence (LII) is a real-time non-intrusive measurement method which uses a pulsed laser to rapidly heat suspended absorbing soot particles to a very high temperature, typically around 4000 K, where they emit visible light [8]. Detection of the emitted light permits the determination of some physical characteristics of the

---

An earlier version of this paper was presented at the IEEE Sensors 2013 Conference, Baltimore MD, and was published in its Proceedings at http://dx.doi.org/10.1109/ICSENS.2013.6688442

Manuscript submitted on 8th October 2015. This research is supported in part by the U.K. Engineering and Physical Sciences Research Council, under Grant EP/J002151/1, “FLITES”.

David McCormick and Krikor B. Ozanyan are with the School of Electrical and Electronic Engineering at the University of Manchester, UK (e-mail: d.mccormick@manchester.ac.uk and k.ozanyan@manchester.ac.uk).

John D. Black was with the Strategic Research Centre, Rolls Royce, Derby, UK and is a Visitor at the University of Manchester, UK (e-mail: John.Black-2@manchester.ac.uk).

Yutong Feng and Johan Nilsson are with the Optoelectronics Research Centre at the University of Southampton, UK (e-mail: y.feng@soton.ac.uk and jn@orc.soton.ac.uk)

Fig.1. Rolls-Royce Gnome engine used in LII experiments (left); view looking down the engine exhaust pipe at the turboshaft heat shield (right)

interacting soot, with studies showing that the resulting LII signal is approximately proportional to the soot volume fraction [9]. LII was first demonstrated for aerosol particles suspended in a gas cell [10] and later came to the attention of the combustion diagnostic community when LII interference was observed in Raman spectroscopy experiments on flames [11]. Later experiments on sooting flames resulted in the development of the first models of LII for soot diagnostics [8], which have been refined over the years [12].

Experimentally, LII has been extensively used in laboratories with sooting flames [13-15] and is an established technique for measurement of soot volume fraction in combustion applications [16-17]. It has been applied to in-cylinder particulate measurement for automotive engines [18-19], and soot sampling in automotive exhausts [20]. In-situ measurement of soot particle concentration in aero-engine exhaust plumes has been demonstrated: in [21] where LII was used to determine radial profiles of soot distribution across the exhaust plume during engine-running conditions; in [22] where a calibrated LII system was used for in-plume soot volume fraction measurement; and in [23] where LII measurements of soot volume fraction on a mid-sized turbofan engine were compared against extractive measurements of soot using the SAESN.

Conventional LII systems for in-situ soot particle sensing in aero-engine exhaust plumes have typically used a Q-switched Nd:YAG laser producing laser pulses with energy around 100 mJ and duration of ~10 ns at a Pulse Repetition Rate (PRR) of the order of ~10 Hz. Consequently, the only excitation wavelengths extensively investigated are the Nd:YAG fundamental at 1064 nm and the second harmonic at 532 nm. Conventional LII systems used in laboratory tests use a light sheet with incandescent light collected at 90° to the laser beam, termed “orthogonal LII”. Access problems in aero-engine test cells mean it is often more practical to collect incandescent light along or at small angles from the path of the laser beam, termed “backward LII”. A true backward configuration only provides measurement of averaged LII along the laser beam path. Off axis LII allows the spatial determination of soot along the laser beam path, and a system with viewing angle as low as 9° between the laser beam path and collection direction has been demonstrated on a small aero-engine [24].

For in-situ soot particle measurement, the main advantages of LII over traditional extractive methods are the increased sensitivity, its non-intrusive nature removing the physical difficulty of sensing within a hot high-velocity flow-field, and a reduction in measurement uncertainties associated with the use of sampling probes and transfer lines. The measurement speed and sensitivity advantages of LII and photoacoustic methods over SAESN for examining extracted gas samples from aircraft engine exhausts are detailed in [25]. There are disadvantages with conventional LII systems because of the low power and short laser pulses, which limit the photon flux reaching the detector and hence sensitivity, whereas low PRR limits the number of measurements obtainable in realistic engine test conditions, thus impacting on signal-to-noise, resolution and frame rate.

Fiber-lasers have been identified as a high power, high PRR source with the facility of variable pulse length and temporal pulse shape, which could address the limitations associated with conventional LII [26]. In-situ soot particle sensing in the exhaust plume of a running aero-engine using fiber-lasers with higher power, longer pulse duration, and higher PRR than conventional LII and has been demonstrated in an earlier paper [27]; this system used an orthogonal configuration with spatially resolved images of the distribution of absorbing particles in the exhaust plume along the laser beam path. Since the laser beam was not expanded into a 2-D light sheet, the spatial resolution in a plane was defined by the camera and the laser beam diameter which, being of the order of 1mm, was small compared to the dimensions of the exhaust plume.

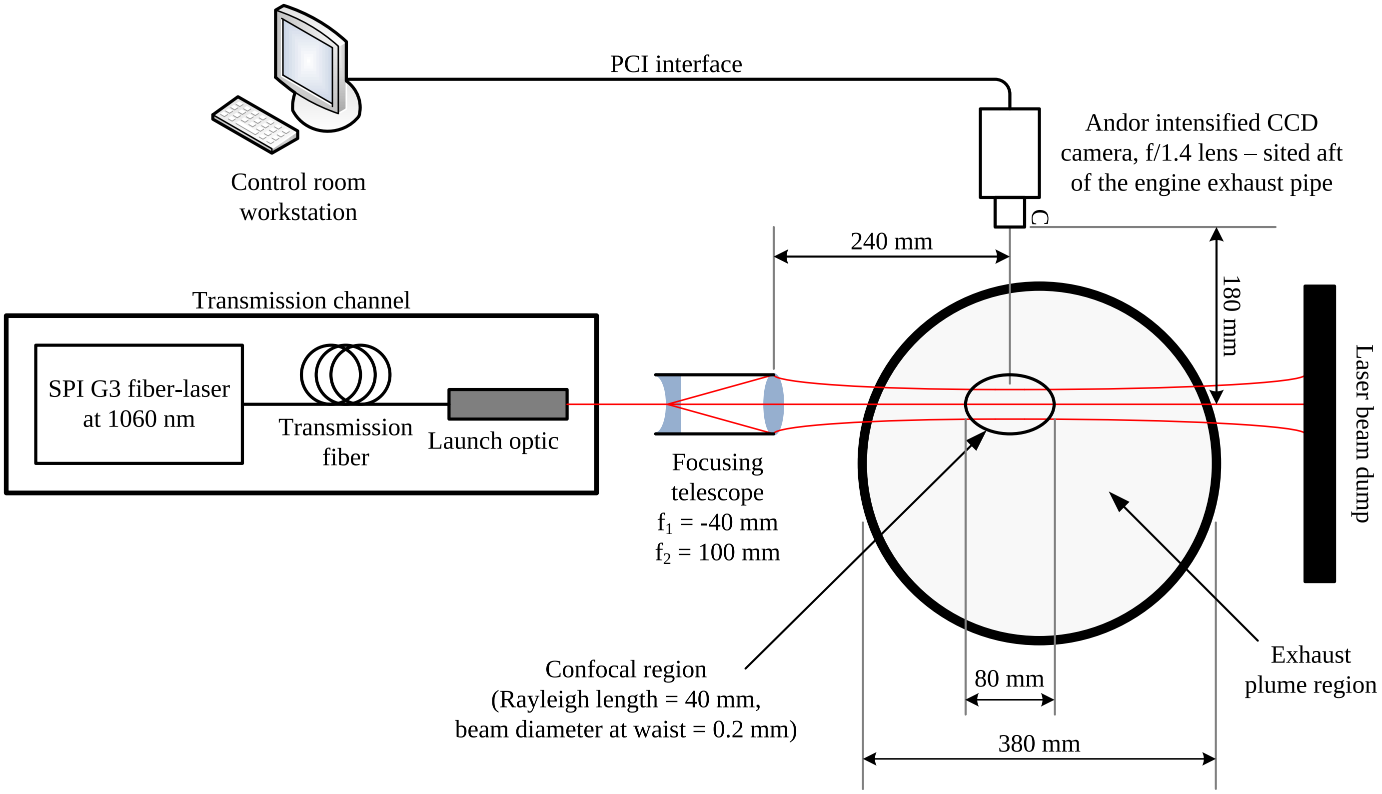

Fig. 2. System configuration for in-situ LII sensing experiments on Rolls-Royce Gnome engine

II. FIBER-LASER INDUCED INCANDESCENCE IN AN AERO-ENGINE EXHAUST PLUME

A. *Experimental Aero-Engine*

The research presented in this paper focuses on investigating in-situ sensing of LII in the exhaust plume of a modified Rolls-Royce Gnome helicopter engine [28], shown in Fig. 1 (left). The engine is located in a closed engine test cell with inlet and outlet at ambient conditions.

The Gnome is a 1950s direct-drive, single-shaft, 10-stage axial flow compressor engine with a two-stage power turbine and annular combustor. It produces a maximum power output of 1119 kW with a mass flow rate of 6.21 kg/s and overall pressure ratio of 8.4:1. For these experiments the engine was modified to remove the power turbine and shaft. This made the engine operate more like a turbojet rather than a turboshaft helicopter engine. In normal engine running conditions, the modifications result in an increase in the temperature and velocity of the engine exhaust plume. The exhaust plume fed into an "engine detuner" which takes the combusted gases out of the test cell (the name detuner comes from the fact that it reduces or "detunes" the noise at the engine output).

Although annular combustors typically produce a uniform combustion profile, the right-angled exhaust pipe with tubular turboshaft heat shield shown in Fig. 1 (right), which would normally surround the power turbine shaft, created an inherently inhomogeneous exhaust plume which is ideally suited to experimental measurements of particulate distributions.

B. *The LII System*

The schematic of the LII system for soot particle sensing experiments on the Rolls-Royce Gnome engine is shown in Fig. 2. The source laser is a commercially available SPI redENERGY^{TM} G3 1060 nm wavelength class 4 fiber-laser capable of providing up to 30 W of average power at PRRs of between 30 kHz and 50 kHz. The laser output is delivered via a 2 m transmission fiber with 35 µm core diameter to a collimating lens launch optics. The laser is weakly focused in the exhaust plume using a focusing telescope (f_1 = -40 mm, f_2 = 100 mm) located at the edge of the Gnome engine exhaust pipe. The laser beam is terminated at a beam dump to minimize the effects of scattered light in the test cell.

The focusing telescope is configured to create a beam waist located at 240 mm from the telescope. Using a "knife-edge scanning" measurement [29], the $1/e^2$ beam waist diameter is measured at approximately 0.2 mm and the Rayleigh length is measured to be 40 mm giving a depth of focus, or confocal region, of 80 mm. The beam attenuation is assumed to be negligible because of low in-plume absorption at 1060 nm. For reasons of optical access around the engine, the confocal region is positioned off-center, both longitudinally down the laser beam and axially across the exhaust plume. All results presented in this paper from the Gnome engine are of LII generated in this region.

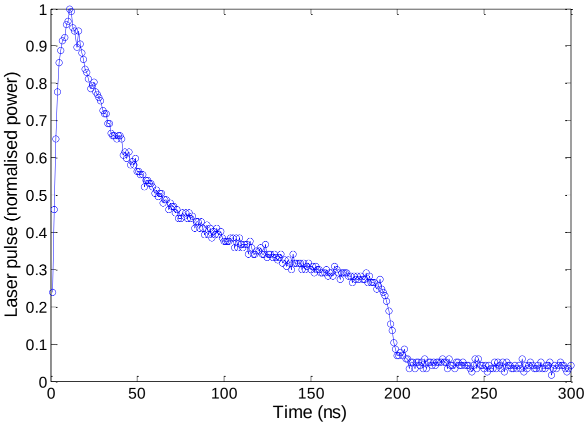

Fig. 3. Trace of 192 ns pulse from SPI laser showing the approximate 10 ns rise time and steady pulse drop-off

To allow for the measurement of spatially resolved absorbing particles along the laser beam path, an orthogonal LII configuration is used with detection channel located aft of the engine exhaust pipe. Wide-field detection of LII is achieved using a COSMICAR C-mount video-camera lens with nominal focal length 16 mm and maximum aperture f/1.4 imaging the LII emission volume on the photocathode of an Andor iStar DH734 gated-intensified CCD camera with a 13 µm pixel size 1024x1024 sensor array. The front element of the lens is positioned 180 mm from the beam waist. Data are transferred to a workstation via a PCI interface and a dedicated PCI-controller where raw data are recorded and time-averaged LII images are generated and analyzed using ImageJ [30]. All images were recorded with the camera operating in CW mode.

The laser was located in the test cell around 2 m from the engine with the transmission channel and camera positioned around the engine on extruded-aluminum frames securely fixed to the test cell floor. The system was controlled from the data acquisition workstation located in the adjacent test cell control room.

III. SOOT PARTICLE SENSING IN AN AERO-ENGINE EXHAUST PLUME BY FIBER-LASER INDUCED INCANDESCENCE

A. *Experimental Configuration*

Soot particle sensing experiments were carried out on the Gnome engine using JetA-1, a kerosene fuel. The experiments were carried out in a closed test bed with the engine inlet and outlet both at ambient ground conditions. The engine plume exhausts to a detuner which is sized to entrain a large excess of air, more than 5-times the amount of air that goes through the engine, to minimize noise at the detuner exit.

The source laser was configured to produce 192 ns pulses, as shown in Fig. 3, generated at a PRR of 30 kHz. The 192 ns pulse is around 20-times longer than that used in conventional LII hence is termed “long-pulsed LII”, and the PRR is around 3-orders of magnitude larger than that used in conventional LII. These attributes are possible in this research because of the use of a fiber-laser.

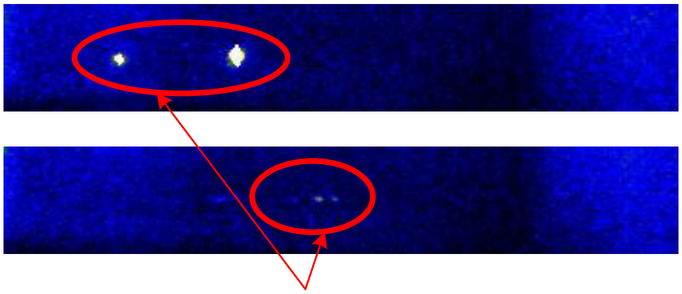

(a) Two instances of observed LII from ambient absorbing particles in the laser beam path

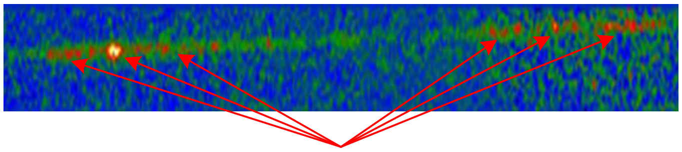

(b) A 60 s cumulative image showing clusters of LII from ambient absorbing particles along the laser beam path

Fig. 4. Images of LII from ambient absorbing particles: two instances of ambient LII in the laser beam path recorded over a 1 s integration time (a); a cumulative image of ambient LII recorded over a 60 s period (b). In all images the laser beam direction is from right to left

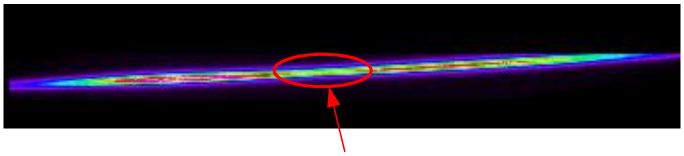

Example of a 1 s in-plume image at 21 W laser power showing lower LII signal around the beam waist due to soot particle vaporization

Fig. 5. Vaporization of soot particles in the laser beam path recorded over a 1 s integration time. The laser beam direction is from right to left

The camera operated in non-triggered mode with variable integration time achieved by altering the camera read out time. By default the camera is configured to read out every 1 s, generating LII images that are integrated over 30000 laser pulses. All images with the engine running are recorded with the camera set to minimum gain level.

B. *Observation of Ambient Absorbing Particles*

Prior to engine runs, LII of ambient absorbing particles in the laser beam path was repeatedly observed with a laser power of 21 W. Fig. 4(a) shows several instances of ambient LII recorded over a 1 s integration time showing non-uniformly distributed absorbing particles, possibly in the form of large agglomerates, located in the laser beam path.

Fig. 4(b) shows a cumulative image of ambient LII recorded over a 60 s period. Clearly visible along the laser beam path are clusters of ambient absorbing particles at different

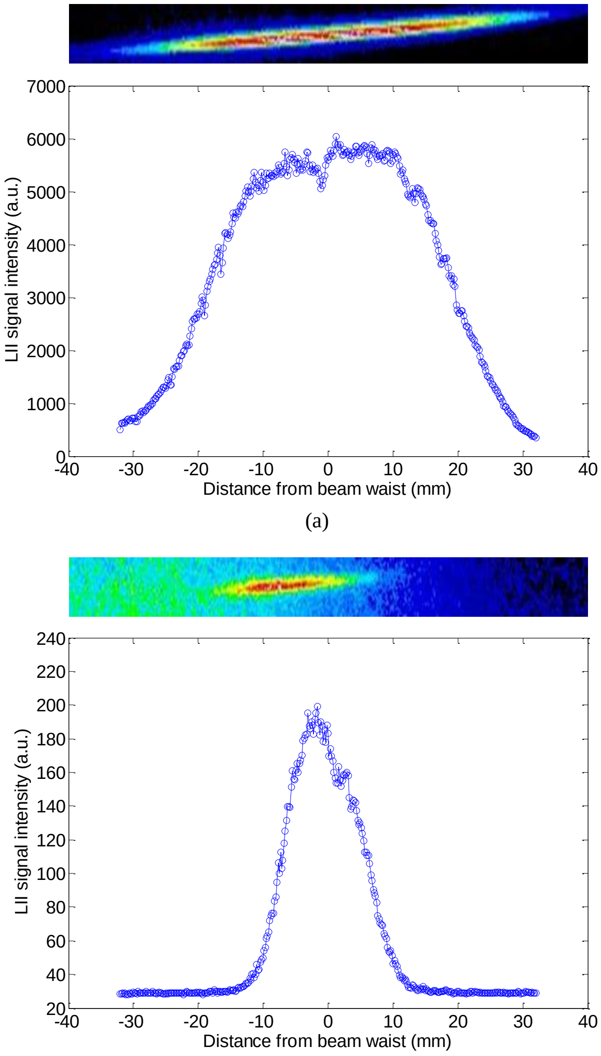

(a)

(b)

Fig. 6. Image of in-plume LII integrated over 1 s (30000 pulses) with plot of signal intensity profile with respect to the beam waist: for 11 W laser power (a); and for 2.2 W laser power (b). In both images the arbitrary units (a.u) are to scale and the laser beam direction is from right to left

locations. This phenomenon has been observed previously [26] and is suspected to be due to ambient particles in the test cell being trapped in the laser beam path forming high density aggregates of absorbing particles. A maximum intensifier gain on the Andor camera of 10^4 was used to record the images shown in Fig. 4.

The observation of LII from ambient absorbing particles is a clear illustration of the sensitivity of using high power, long pulses fiber-lasers for sensing of absorbing particles.

C. *In-plume Soot Particle Sensing*

The laser power was varied experimentally to determine the test range for in-plume experiments. The ability to generate LII from absorbing particles depends on the laser fluence which describes the energy per unit area along the beam. Below a certain laser fluence threshold the absorbing particles do not reach a sufficiently high temperature to emit visible light detectable by the camera. As the laser fluence increases beyond this threshold, the absorbing particles reach a temperature such that they emit visible light until the particles reach a temperature where they begin to vaporize. At power levels above 2.2 W, in-plume LII was observed which increased proportional to the laser power. Beyond 11 W, soot particle vaporization, indicated by a lower LII signal around the beam waist was observed; this was particularly noticeable at laser powers above 20 W, as shown in Fig. 5, where vaporization can be clearly seen for laser power of 21 W. The peak focal fluence in this region was calculated as 1.21 J/cm².

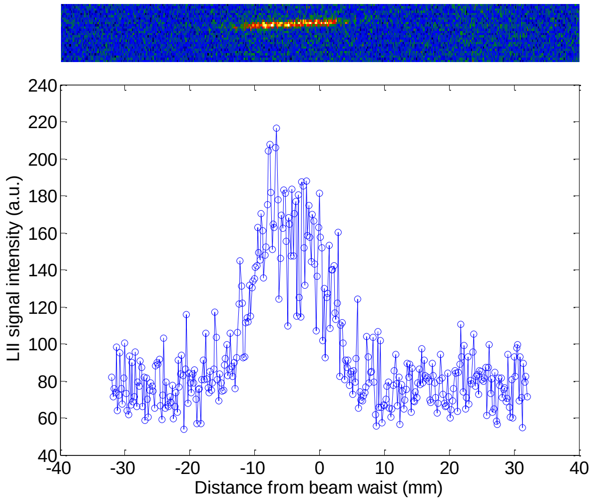

Fig. 7. Image of in-plume LII integrated over 0.1 s (300 pulses) with plot of signal intensity profile with respect to the beam waist for 2.2 W laser power. The a.u is to scale with the images in Fig. 6 and the laser beam direction is from right to left

Results for the in-plume sensing of LII from soot particles are shown in Fig. 6. Images for laser powers of 11 W (a) and 2.2 W (b) integrated over 1 s (30000 pulses) are shown with the Gnome engine running at 19475 rpm. At 11 W the peak focal fluence is 0.64 J/cm² and at 2.2 W the peak focal fluence is 0.13 J/cm². From the LII images the signal intensity along the laser beam is plotted with respect to the beam waist.

Higher laser power results in a more intense LII signal across the confocal region. This is evident from the peak measured LII at the beam waist, where an increase in laser power from 2.2 W to 11 W results in a 30-times increase in the LII signal measured on the camera, as well as broadening of the observed LII along the laser beam path. From the fluence curve in [22] for LII generated with a ~10 ns pulse laser, the expectation is that there would be less signal at 11 W than at 2.2 W due to vaporization of the soot particles at the higher fluence. However, with this long-pulsed fiber-laser vaporization appears to occur at higher fluences, typically beyond 0.65 J/cm², and 2.2 W appears to be close to lower threshold for generating LII hence may not be in the linear region of the fluence curve. The LII-fluence characteristic of long-pulsed lasers requires further investigation.

Asymmetry of the cross-plume profile is evident at lower powers. Previous studies have suggested that such asymmetry can occur in unmixed flow engines because large refractive index changes between the ambient air in the test cell and the

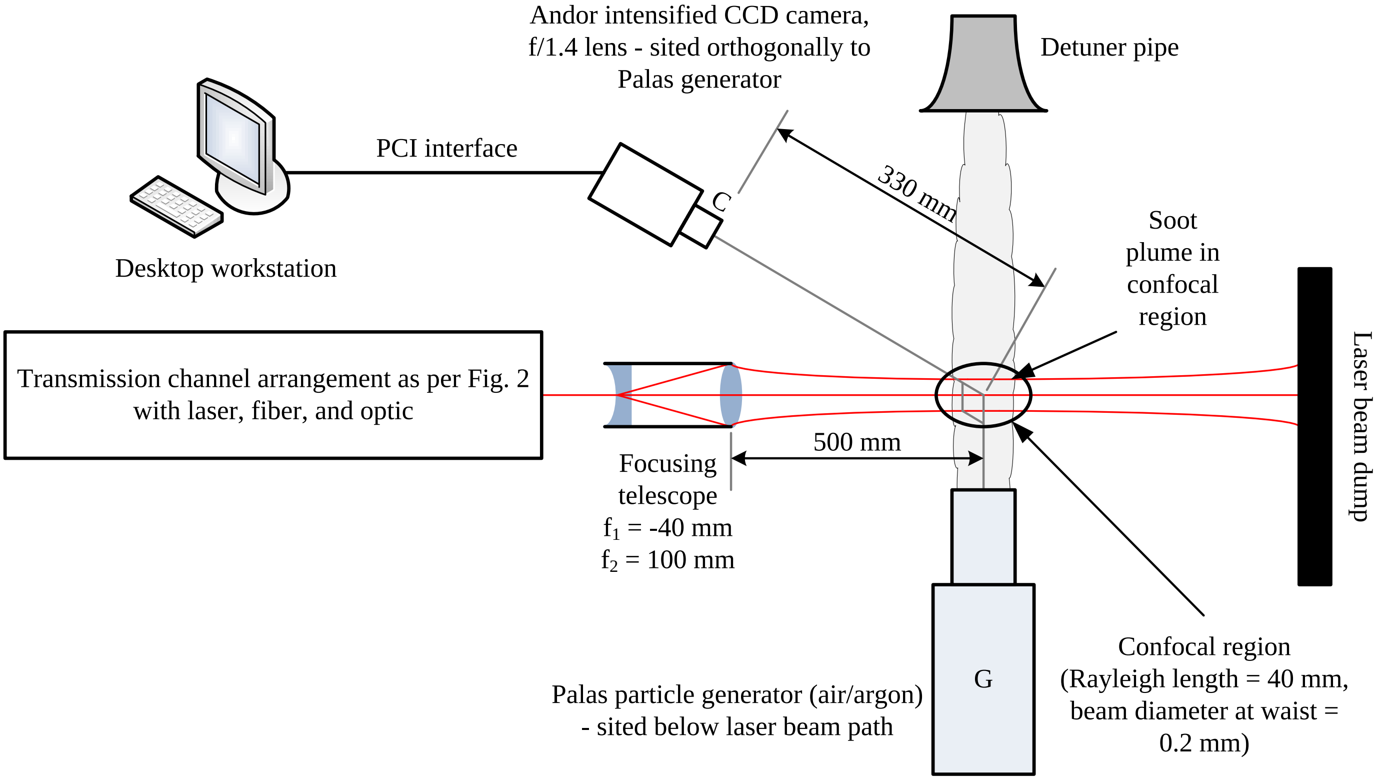

Fig. 8. System configuration for LII sensing experiments in a controlled laboratory

hot exhaust gases result in significant beam steering at the air-plume boundary [21]. This phenomenon is less evident in mixed flow where the high bypass ratio produces overall lower temperatures and hence less observable beam steering [23]. These results from a unmixed flow engine offer some support to previous observations, however definitive conclusion are difficult to draw because of the effects of CO_2 and water concentrations in the plume, both of which can have an effect on the refractive index.

To increase the data acquisition rate of the LII system the integration time for acquiring the images was reduced by altering the read-out time from the Andor camera. Fig. 7 shows the LII images and profile for a laser power of 2.2 W integrated over 0.01 s (300 pulses) with the Gnome engine running at 19475 rpm.

The general shape of the LII profile is similar to the 1 s integration profile (Fig. 6b) with peak LII signal intensity of around 200, asymmetrically positioned around 5-10 mm to the left of the beam waist. The most obvious difference is the significant increase in noise on the data because of reduced signal sampling. Reducing the integration time further causes the noise to dominate the data.

Further work will consider configuring the camera in gated-mode triggered from the laser pulse. This will permit acquisition of LII from individual laser pulses in an attempt to further reduce the integration time and hence increase the data acquisition rate.

IV. TOWARDS MEASUREMENT OF SOOT VOLUME FRACTION

A. *Laboratory LII System*

The schematic of the laboratory LII system for controlled soot particle sensing experiments is shown in Fig. 8. The design of this system is based on the LII system used for soot particle sensing experiments on the Rolls-Royce Gnome engine discussed in section II.B and shown in Fig. 2. It uses the same SPI redENERGY^{TM} G3 source laser, transmission fiber, launch optic, and focusing telescope on the transmission channel; and Andor iStar CCD camera with COSMICAR C-mount video-camera lens on the detection channel.

The focusing telescope is configured to create a beam waist located at 500 mm from the telescope with the $1/e^2$ beam waist diameter measured at approximately 0.2 mm. The front element of the camera lens is positioned 330 mm from the beam waist in an orthogonal LII configuration. The laser beam is terminated at a beam dump to minimize the effects of scattered light in the laboratory. The camera is interfaced to a workstation via a PCI interface where raw data are recorded and analyzed. All images were recorded with the camera operating in CW mode

The source of absorbing particles is a Palas GfG1000 Graphite Aerosol Generator sited directly below the beam waist. This device produces carbon particles of similar size to those found in diesel engine exhausts by generating a flashover between two carbon electrodes in an argon flow. Particle volume fraction is varied in a controlled manner by

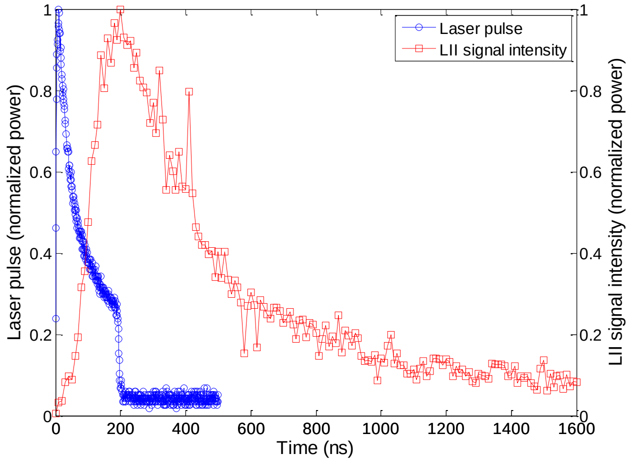

Fig. 9. Time resolved LII results showing the 192 ns pulse from the SPI laser (circles/blue) and the resulting time-resolved normalized power profile of the induced LII signal (squares/red) over a 1600 ns measurement window

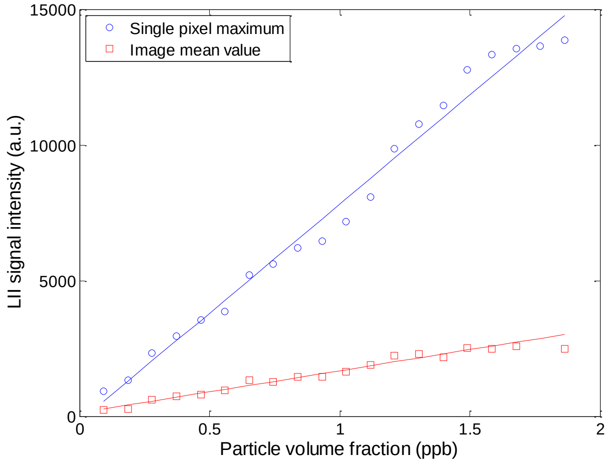

Fig. 10. Measured on a 26x10 pixel LII image, peak LII signal intensity as a function of the particle volume fraction from the Palas GfG 1000 for a single point maximum (circles/blue) and image mean (squares/red)

diluting the argon flow with air downstream of the arc to produce particles with diameter in the 10-100 nm range at concentrations greater than 10^7/cm³. The plume is exhausted through a detuner pipe situated above the laser beam path.

B. Time-Resolved LII

Using the laboratory system in Fig. 8, measurements of time-resolved LII data were taken. Fig. 9 shows the time resolved LII signal intensity measured over a 1600 ns window normalized to the 192 ns SPI laser pulse (shown previously in Fig. 3). The LII signal builds up after the initial laser pulse and peaks at around 200 ns, decaying to 1/*e* of the peak power after around 500 ns. The 10-90% rise time is 110 ns and the 90-10% fall time is 1080 ns. This time-resolved characteristic is consistent with LII responses using conventional Q-switched Nd:YAG lasers discussed in the literature and suggests that this laser would be suitable in applications requiring time-resolved measurements. Whilst the time-resolved characteristic is consistent with conventional laser results, further work is required to understand the LII process for laser pulse lengths of the order of ~200 ns to establish a new model of long-pulsed LII.

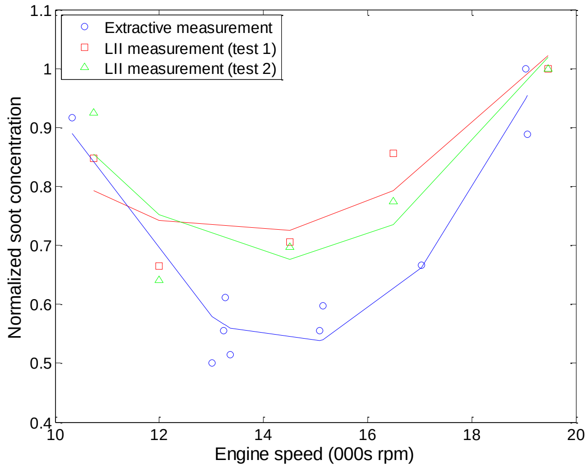

Fig. 11. Comparison of normalized soot concentration measurements from the Gnome engine using LII (squares/red and triangle/green) and an extractive measurement using SAESN [6] (circles/blue) for different engine speeds between 10330 rpm and 19475 rpm

C. Calibration for Soot Measurement

The GfG100 was calibrated using a commercial Artium LII300 extractive system. To measure particle volume fraction using the LII300 system, a small gas sample is collected into a chamber and orthogonal LII is used to measure the LII signal intensity. The signal intensity is then calibrated to the particle volume fraction in method similar to that detailed in [31]. Fig. 10 shows the linear correlation of LII collected in this arrangement with particle volume fraction. The image single point maximum and image mean for a 26x10 pixel image of LII is shown to be linear with the particle volume fraction produced from a calibrated particle generator. This is a critical result for in-plume measurement of soot as it demonstrates that for long-pulsed lasers, as with short-pulsed lasers, the LII signal intensity is linear with the soot concentration.

Whilst this result is crucial in developing a calibration system, it should be stressed that the carbon particles are not engine soot and therefore further work is required to determine the accuracy of this calibration method for certification purposes.

D. Comparison of Engine LII with Extractive Measurements

Using the LII data from the Gnome engine presented in part III, the data were calibrated for soot concentration and compared to extracted gas samples using a TSI 3080-series scanning mobility particle sizer instrument with TSI 3081 differential mobility analyzer. Fig. 11 shows a normalized comparison of soot concentration measured by LII with extractive measurements. Both techniques show the same trend in measured soot concentration across a range of engine speeds. At low engine speed, around 10500 rpm, the measured soot concentration is high at around 0.85 to 0.93 and the difference between LII and extractive measurements is around 4.4%. At medium engine speeds, between 12000 rpm and 16000 rpm, the measured soot concentration drops off to between 0.5 and 0.7 and the discrepancy between LII and extractive measurements increases to around 15-18%. At engine speeds greater than 16000 rpm, the measured soot concentration increases again to between 0.87 and 1.00 and the discrepancy drops back again to around 6%. Across a range of engine speeds these results show that measurements of soot concentration by LII are consistent with extractive data obtained using the current industry standard method for certification. Calibration is still a problem because of the need for a reproducible and reliable source of post-flame soot which may account for the observed increased differences in measured soot concentration between the two methods at lower concentrations.

This work should be viewed as an initial demonstration that this type of low-cost fiber-laser, normally used for marking materials, can be used for non-intrusive measurement of soot particles in an aero-engine exhaust plume. LII using Q-switched Nd:YAG lasers is fairly well established for this application and LII on extracted gas samples may well replace the current filter paper reflectance method for engine certification.

V. CONCLUSION

In-situ sensing of LII from absorbing soot particles has been demonstrated using high power, long pulsed, high PRR fiber-lasers in the exhaust plume of a gas turbine engine. Images of ambient and in-plume LII generated from a 1060 nm, 192 ns pulse duration, 30 kHz PRR fiber-laser have been presented. The reduction of the integration time has been considered and its impact on imaging performance and data acquisition rates has been discussed with further work identified. A representative LII laboratory system has been developed to investigate the time-resolved LII characteristics and the dependence of the LII signal intensity on the soot concentration. Results of soot concentration by LII have been compared with results from extractive measurements with good agreement across a range of engine conditions.

The demonstration of LII in the exhaust of a running aero-engine using fiber-lasers is the first step in the development of emission measurement for aero-engine combustion diagnostics without the requirement for engine mounted sensors. By scanning the laser beam in an auto-projection tomography arrangement as discussed in [32], a 2-D image of soot distribution in the exhaust plume can be generated, giving access to information about the behavior of the engine combustor and the mixing of the core and bypass streams, which is currently unobtainable. Detection of LII by viewing a focused beam at 90° is unconventional and further laboratory experiments are required to establish laser power dependence and the optimum configuration for practical measurement on aero-engine testbeds.

REFERENCES

[1] E.J. Highwood and R.P. Kinnersley, “When smoke gets in our eyes: The multiple impacts of atmospheric black carbon on climate, air quality and health,” *Environ. Int.*, vol. 32, no. 4, pp. 560-566, 2006.

[2] C. Arden Pope III, R.T. Burnett, M.J. Thun, E.E. Calle, D. Krewski, K. Ito, G.D. Thurston, “Lung cancer, cardiopulmonary mortality, and long-term exposure to fine particulate air pollution,” *J. Am. Med. Assoc.*, vol. 287, no. 9, pp. 1132-1141, 2002.

[3] J.T. Houghton, Y. Ding, D.J. Griggs, M. Noguer, P.J. van der Linden, D. Xiaosu (eds.), *Climate Change 2001: The Scientific Basis*. Cambridge, Cambridge University Press, 2001, vol. 881.

[4] *Conv. Int. Civil Aviation*, Annex 16 Volume II, 2006 (9th Edition).

[5] L.C. Law, “Recent advancements in aircraft engine health management (EHM) technologies and recommendations for the next step,” in *Proc. ASME Turbo Expo 2005: Power for Land, Sea, and Air*, Reno, NV, 2005, pp. 683-695.

[6] *Aircraft Gas Turbine Engine Exhaust Smoke Measurement*, SAE ARP1179 Rev. D, 2011.

[7] K. Schäfer, J. Heland, D.H. Lister, C.W. Wilson, R.J. Howes, R.S. Falk, E. Lindermeir, M. Birk, G. Wagner, P. Haschberger, M. Bernard, O. Legras, P. Wiesen, R. Kurtenbach, K.J. Brockmann, V. Kriesche, M. Hilton, G. Bishop, R. Clarke, J. Workman, M. Caola, R. Geatches, R. Burrows, J.D. Black, P.Hervé, J. Valley, “Nonintrusive optical measurements of aircraft engine exhaust emissions and comparison with standard intrusive techniques,” *Appl. Opt.*, vol. 39, no. 3, pp. 441-455, 2000.

[8] L.A. Melton, “Soot diagnostics based on laser heating,” *Appl. Opt.*, vol. 23, no. 13, pp. 2201-2208, 1984.

[9] H. Bladh, J. Johnsson, P-E. Bengtsson, “On the dependence of the laser-induced incandescence (LII) signal on soot volume fraction for variations in particle size,” *Appl. Phys. B*, vol. 90, no. 1, pp. 109-125. Jan. 2008.

[10] R.W. Weeks and W.W. Duley, “Aerosol-particle sizes from light emission during excitation by TEA CO_2 laser pulses,” *J. Appl. Phys.*, vol. 52, no. 10, pp. 4661-4662, 1974.

[11] A.C. Eckbreth, “Effects of laser-modulated particulate incandescence on Raman scattering diagnostics,” *J. Appl. Phys.*, vol. 48, pp. 4473-4479, 1977.

[12] H.A. Michelsen, “Understanding and predicting the temporal response of laser-induced incandescence from carbonaceous particles,” *J. Chem. Phys.*, vol. 118, pp. 7012-7045, 2003.

[13] C.R. Shaddix, K.C. Smyth, “Laser-induced incandescence measurements of soot production in steady and flickering methane, propane, and ethylene diffusion flames,” *Combust. Flame*, vol. 107, no. 4, pp. 418-452, 1996.

[14] D.R. Snelling, K.A. Thomson, G.J. Smallwood, Ö.L. Gülder, “Two-dimensional imaging of soot volume fraction in laminar diffusion flames,” *Appl. Opt.*, vol. 38, no. 12, pp. 2478-2485, 1999.

[15] P. Desgroux, X. Mercier, B. Lefort, R. Lemaire, E. Therssen, J.F. Pauwels, “Soot volume fraction measurement in low-pressure methane flames by combining laser-induced incandescence and cavity ring-down spectroscopy: Effect of pressure on soot formation,” *Combust. Flame*, vol. 155, no. 1-2, pp. 289-301, 2008.

[16] R.L. Vander Wal and K.J. Weiland, “Laser-induced incandescence: development and characterization towards a measurement of soot volume fraction,” *Appl. Phys. B*, vol. 59, no. 4, pp. 445-452, 1994.

[17] B. Axelsson, R. Collins, P-E. Bengtsson, “Laser-induced incandescence for soot particle size and volume fraction measurements using on-line extinction calibration,” *Appl. Phys. B*, vol. 72, no. 3, pp. 367-372, 2001.

[18] B.F. Kock, B. Tribalet, C. Schulz, P. Roth, “Two-color time-resolved LII applied to soot particle sizing in the cylinder of a Diesel engine,” *Combust. Flame*, vol. 147, no. 1-2, pp. 79-92, 2006.

[19] B. Bougie, L.C. Ganippa, A.P. van Vliet, W.L. Meerts, N.J. Dam, J.J. ter Meulen, “Soot particulate size characterization in a heavy-duty diesel engine for different engine loads by laser-induced incandescence,” *P. Combust. Inst.*, vol. 31, no. 1, pp. 685-691, 2007.

[20] M.K. Case, D.L. Hofeldt, “Soot mass concentration measurements in diesel engine exhaust using laser-induced incandescence,” *Aerosol Sci. Tech.*, vol. 25, no. 1, pp. 46-60, 1996.

[21] J.D. Black, J. Delhay, M.P. Johnson, “In-situ laser-induced incandescence of soot in large civil aero-engine exhausts,” in *Proc. 26th AIAA Aerodynamic Measurement Technology and Ground Testing Conf.*, Seattle, WA, 2008, pp. AIAA Paper 2008-4265.

[22] J. Delhay, P. Desgroux, E. Therssen, H. Bladh, P-E. Bengtsson, H. Hönen, J.D. Black, I. Vallet, "Soot volume fraction measurement in aero-engine exhausts using extinction-calibrated backward laser-induced incandescence," *Appl. Phys. B: Laser and Optics*, vol. 95, no. 4, pp. 825-838, 2009.

[23] J. D. Black and M. P. Johnson, "In-situ laser-induced incandescence of soot in an aero-engine exhaust: Comparison with certification style measurements," *Aerosp. Sci. Technol.*, vol. 14, no. 5, pp. 329-327, 2010.

[24] T. P. Jenkins, J. L. Bartholomew, P. A. DeBarber, P.Yang, J. M. Seitzman, R .P. Howard, "A laser-induced incandescence system for measuring soot flux in aircraft engine exhausts" in Proc. AIAA/ASME/SAE/ASEE Joint Propulsion Conference, Indianapolis, IN, 2002, AIAA paper 2002-3736.

[25] *Procedure for the Continuous Sampling and Monitoring of Non-Volatile Particle Emissions from Aircraft Turbine Engines*, SAE AIR6241, 2013.

[26] J.D. Black, "Fiber lasers as a source for laser-induced incandescence in practical applications", in *Proc. Laser Applications to Chemical, Security and Environmental Analysis Conf.*, San Diego, CA, 2010, pp. Paper LWB5.

[27] D. McCormick, J.D. Black, K.B. Ozanyan, Y. Feng, "In-Situ Soot Particle Sensing in an Aero-Engine Exhaust Plume," in *Proc. IEEE Sensors 2013 Conf.*, Baltimore, MD, 2013, pp. 1254-1257.

[28] Flight International, "Turbine Engines of the World" in British European Aerospace/Preview of 1973, London: IPC Business Press Ltd, 1973, pp.36.

[29] A.H. Firester, M.E. Heller, P. Sheng, "Knife-edge scanning measurements of subwavelength focused light beams," *Appl. Opt.*, vol.16, no. 7, pp. 1971-1974, 1977.

[30] W. Rasband, (2014, May). ImageJ software. *National Institute of Health (NIH)*. Available: http://imagej.nih.gov/ij/index.html.

[31] G. Smallwood, D. Clavel, D. Gareau, R. Sawchuk, D.R. Snelling, P.O. Witze, B. Axelsson, W.D. Bachalo, Ö.L. Gülder, "Concurrent Quantitative Laser-Induced Incandescence and SMPS Measurements of EGR Effects on Particulate Emissions from a TDI Diesel Engine", SAE Technical Paper 2002-01-2715, 2002.

[32] P. Wright, D. McCormick, K. Ozanyan, M. Johnson, J. Black, E. Fisher, A. Chighine, N. Polydorides, H. McCann, Y. Feng, K. Khan, P. Bastock, J. Fuqiang., D. Hewak, J. Nilsson, M. Lengden, D. Wilson, I. Armstrong, T. Benoy, W. Johnstone, "Progress towards non-intrusive optical measurement of gas turbine exhaust species distributions," in *Proc. IEEE Aero Conf. 2015.*, Big Sky, MT, 2015, pp. 1-14.

David McCormick (M'13) received the B.Eng. degree in electronic systems engineering and the Eng.D degree in electrical and electronic engineering from the University of Manchester, UK, in 2006 and 2011 respectively. He also received the Pg.Dip degree in management sciences from Manchester Business School in 2008.

Following 10-years working in industry for several large engineering organizations and UK-based SMEs, between 2012 and 2014 he was a postdoctoral researcher working on the EPSRC-funding FLITES project. Since 2014, he has been a Lecturer with the School of Electrical and Electronic Engineering at the University of Manchester, UK. His research interests include aerospace combustion diagnostics, optical and electrical tomography and development of novel industrial sensors and instrumentation.

Dr. McCormick is a Chartered Engineer with the Institution of Engineering and Technology and was elected a Whitworth Senior Scholar in 2012. His awards include the Worshipful Company of Scientific Instrument Makers Beloe Fellowship 2013-14, the Whitworth Visionary Award 2012 and a Whitworth Senior Scholarship Award (both from the Institution of Mechanical Engineers).

John D. Black received B.Sc. and Ph.D. degrees in chemistry from the University of Glasgow, in 1971 and 1975.

Following postdoctoral posts at Universities of Southampton and Southern California, he joined Rolls-Royce plc in 1981 and worked in their Strategic Research Centre until retirement in 2012. He was awarded a Royal Society Industry Fellowship in 2009 and spent the following two years on secondment at University of Manchester.

Dr. Black is a member of the SAE E31 committee which advises ICAO on methods of measurement of aero-engine exhaust emissions. He pioneered the application of LII for in-situ soot particle measurement in aero-engine exhausts through three EU funded collaborative programs and instigated the current UK FLITES project for non-intrusive mapping of aero-engine exhaust emissions.

Yutong Feng was born in Baoji, China, in 1982. He received the B.S. degree in applied physics from Northwest University, Xi'an, China, in 2004 and the Ph.D. degree in optical engineering from Shanghai Institute of Optics and Fine Mechanics, Chinese Academy of Sciences, Shanghai, China, in 2009. He is currently a Postdoctoral Research Fellow at the Optoelectronics Research Centre, University of Southampton, UK.

From 2009 to 2012, he was a Research Assistant at North China Research Institute of Electro-Optics, Beijing, China. His research interest includes high power fibre lasers and amplifiers, nonlinear fibre optics, systems and applications aspects.

Johan Nilsson is a Professor at the Optoelectronics Research Centre (ORC), University of Southampton, England. In 1994, he received a doctorate in Engineering Science from the Royal Institute of Technology, Stockholm, Sweden, for research on optical amplification. Since then, he has worked on optical amplifiers and amplification in lightwave systems, optical communications, and guided-wave lasers, first at Samsung Electronics and later at ORC. His research has covered system, fabrication, and materials aspects of guided-wave lasers and amplifiers, and in particular device aspects of high power fiber lasers and erbium-doped fiber amplifiers.

He is leading ORC's high-power fiber-laser group which, in recent years, demonstrated a number of world-firsts and world-records in the field, including the first single-mode kW fiber-laser and the first cladding-pumped fiber Raman laser. He has published nearly 400 scientific articles and has taught several short courses on fiber-lasers and amplifiers. He is a fellow of the OSA, a life member of the SPIE, a consultant to, and co-founder of, SPI Lasers, and a member of the advisory board of the Journal of the Optical Society of Korea. In addition, he was guest editor of two issues on high-power fiber-lasers in IEEE Journal of Selected Topics in Quantum Electronics in 2009. He has also been active in the organization of several conferences and meetings, and is a former chair of the Laser Science and Engineering technical group in OSA's Science and Engineering Council. At present he is a member of the technical program committee of the Europhoton and the Optical Instrument and Technology conference.

Krikor B. Ozanyan (M'95-SM'03) received the M.Sc. degree in engineering physics (semiconductors) and the Ph.D.

degree in solid-state physics from the University of Sofia, Sofia, Bulgaria, in 1980 and 1989, respectively.

He has held previous academic and research posts with the University of Sofia, The Norwegian Institute of Technology, Trondheim, Norway, the University of Hull, Hull, U.K., and the University of Sheffield, Sheffield, U.K., working on projects ranging from Brewster-angle mid-IR spectroscopic ellipsometry and electron confinement in quantum wells and barriers, to the demonstration of the lasing at 333 nm from strained MQW ZnCdS/ZnS structures and in-situ real-time optical monitoring of growth of III–V semiconductors in MBE and MOCVD reactors. His current research interests include photonic sensors and indirect imaging (tomography) by optical modalities, signal processing for optical experiments, and spectroscopy with ultrafast laser sources. He is currently the Head of sensors, imaging and signal processing with the University of Manchester and a Visiting Professor with the University of Bergen, Bergen, Norway.

Prof. Ozanyan is a Fellow of the Institute of Engineering and Technology, (U.K., formerly IEE) and the Institute of Physics, U.K. He was a Distinguished Lecturer of the IEEE Sensors Council from 2009 to 2010, a Guest Editor of the IEEE Sensors Journal Special Issues “Sensors for Industrial Process Tomography” in 2005 and “THz Sensing: Materials, Devices and Systems” in 2012. He is currently Editor-in-Chief of the IEEE Sensors Journal.